

## Supporting Information

### Acid-Directed Morphology Control of Molybdenum Carbide Embedded in Nitrogen Doped Carbon Matrix for Enhanced Electrocatalytic Hydrogen Evolution

Jing Wang <sup>a</sup>, Siwei Li <sup>a\*</sup>, Jing Hu <sup>a</sup>, Siqi Niu <sup>a</sup>, Yuzhi Li <sup>a</sup>, Ping Xu <sup>a, b\*</sup>

<sup>a</sup> *MIIT Key Laboratory of Critical Materials Technology for New Energy Conversion and Storage, School of Chemistry and Chemical Engineering, Harbin Institute of Technology, Harbin 150001, China*

<sup>b</sup> *Guangdong Provincial Key Laboratory of Energy Materials for Electric Power, Shenzhen 518055, China*

\* E-mail: p xu@hit.edu.cn; swli@hit.edu.cn

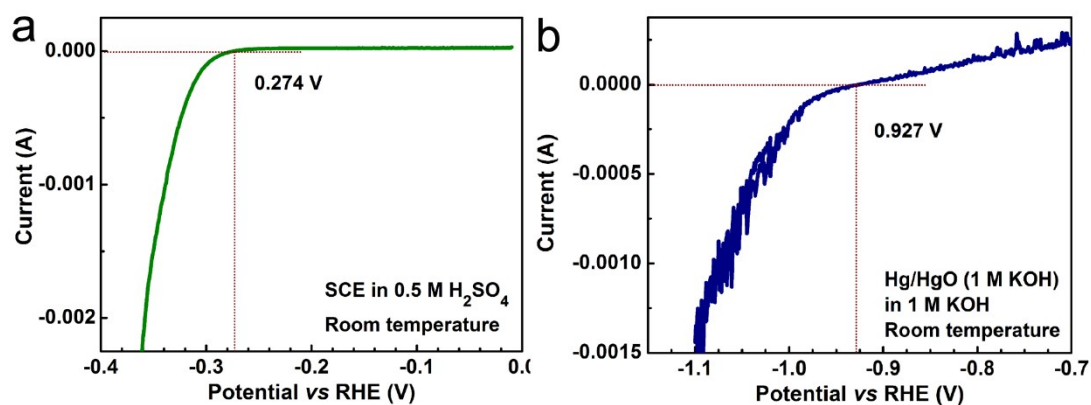


**Fig. S1** Calibration curves of reference electrodes. (a) saturated calomel electrode (SCE) in 0.5 M H<sub>2</sub>SO<sub>4</sub> solution and (b) Hg/HgO (1.0 M KOH) electrode in 1.0 M KOH at room temperature.

Before electrochemical measurement, all the reference electrodes should to be calibrated to guarantee the veracity and reliability of test results <sup>S1</sup>. In the calibration process, Pt sheet (purchased from Aldrich) were used as working and counter electrodes, SCE and Hg/HgO (1.0 M KOH) electrode were applied as reference electrodes in 0.5 M H<sub>2</sub>SO<sub>4</sub> solution and 1.0 M KOH, respectively. Before calibration, H<sub>2</sub> was led continuously into the solution for 30 min to saturate the solution with hydrogen. Then, calibration curves in 0.5 M H<sub>2</sub>SO<sub>4</sub> and 1.0 M KOH were obtained with a scan rate of 1 mV/s at room temperature, as shown in Figure S1. The corrected potentials of SCE and Hg/HgO electrode are 0.274 V and 0.927 V vs RHE, respectively.

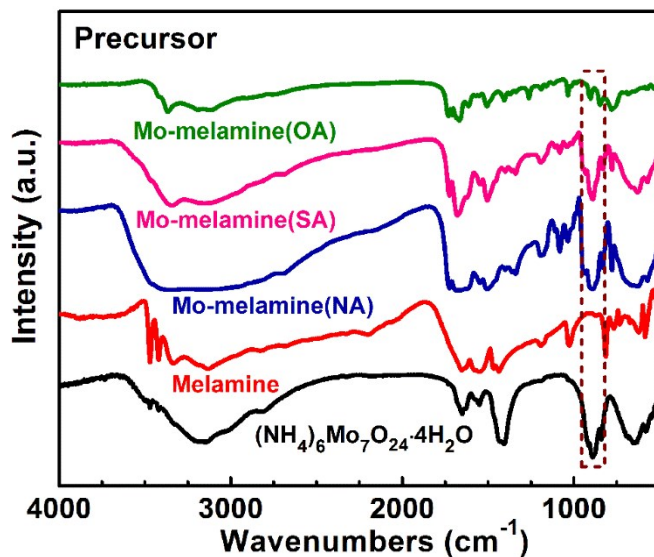


**Fig. S2** FTIR spectra of as-prepared Mo-melamine(OA), Mo- melamine (SA), Mo-melamine (NA) precursors.

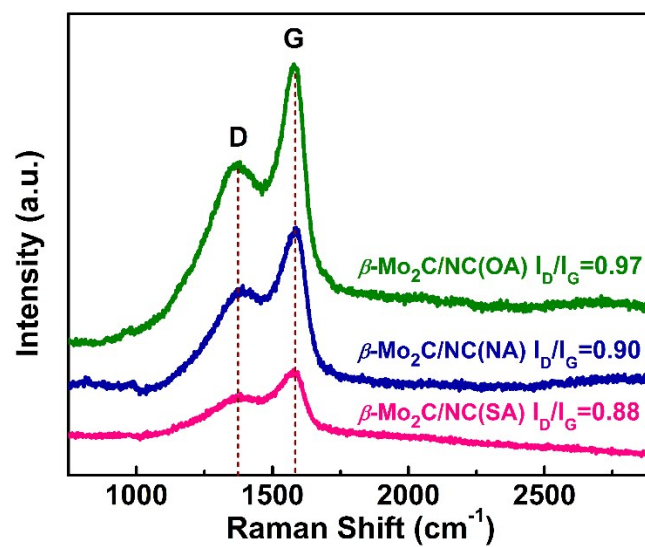


**Fig. S3** Raman spectra for as-prepared  $\beta\text{-Mo}_2\text{C/NC(OA)}$ ,  $\beta\text{-Mo}_2\text{C/NC(SA)}$ ,  $\beta\text{-Mo}_2\text{C/NC(NA)}$ .

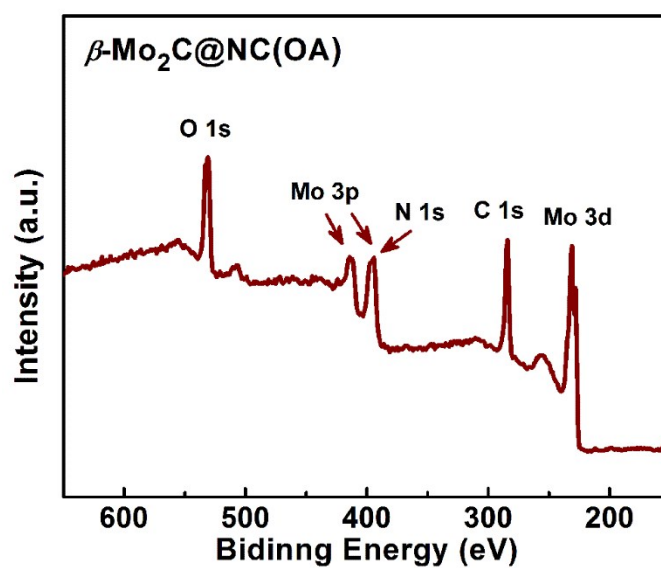


**Fig. S4** Survey XPS spectrum of  $\beta\text{-Mo}_2\text{C/NC(OA)}$ .

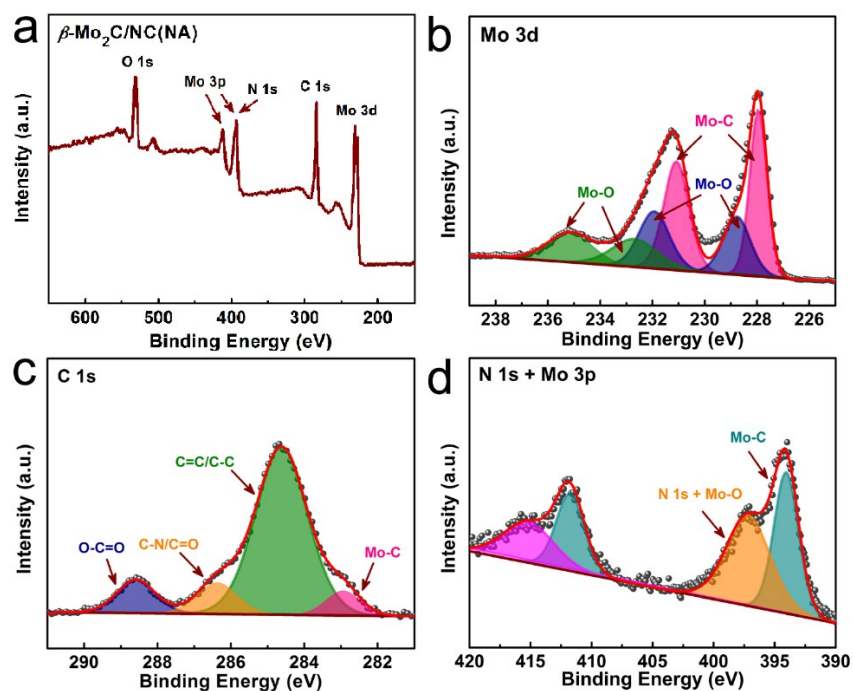


**Fig. S5** (a) Survey XPS spectrum of  $\beta$ -Mo<sub>2</sub>C/NC(NA); High-resolution XPS spectra of (b) Mo 3d, (c) C 1s and (d) N 1s - Mo 3p of  $\beta$ -Mo<sub>2</sub>C/NC(NA).

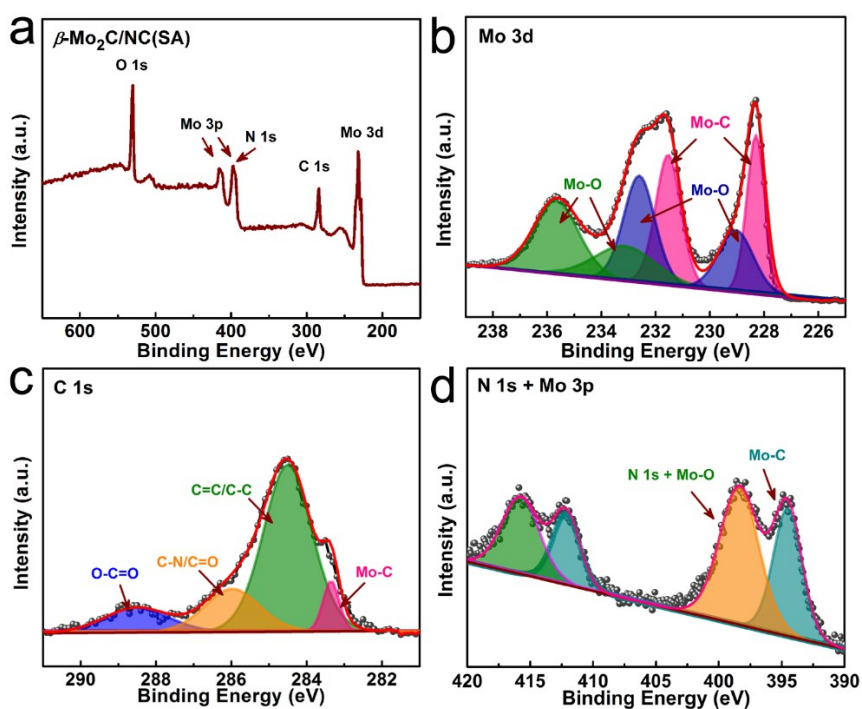


**Fig. S6** (a) Survey XPS spectrum of  $\beta$ -Mo<sub>2</sub>C/NC(SA); High-resolution XPS spectra of (b) Mo 3d, (c) C 1s and (d) N 1s-Mo 3p of  $\beta$ -Mo<sub>2</sub>C/NC(SA).

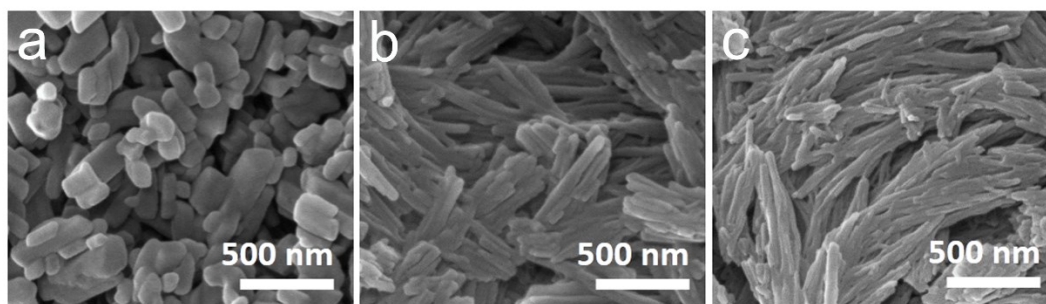


**Fig. S7** SEM images of precursor for (a)  $\beta$ -Mo<sub>2</sub>C/NC(OA), (b)  $\beta$ -Mo<sub>2</sub>C/NC(NA) and (c)  $\beta$ -Mo<sub>2</sub>C/S-NC(SA)

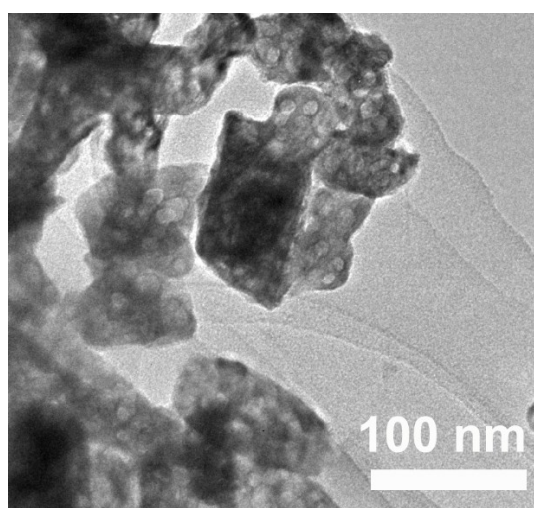


**Fig. S8** High-magnified TEM images of  $\beta$ -Mo<sub>2</sub>C/NC(OA).

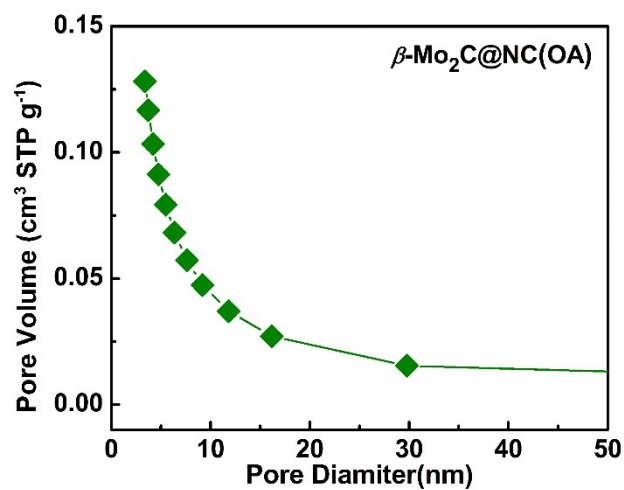


**Fig. S9** Pore size distribution diagram of as-prepared  $\beta$ -Mo<sub>2</sub>C/NC(OA).

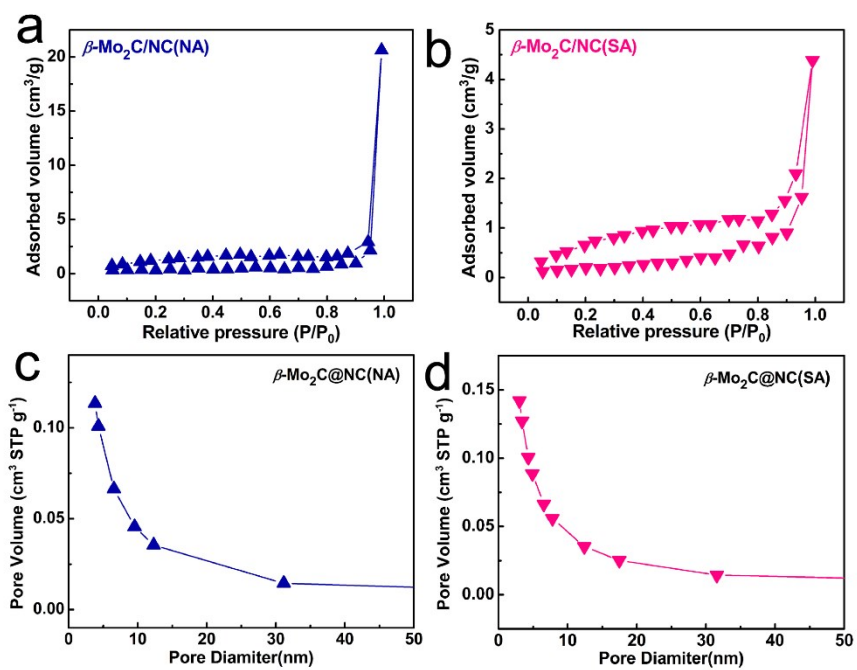


**Fig. S10** (a, b) Nitrogen absorption and desorption diagrams and (c, d) pore size distribution diagrams of as-prepared  $\beta$ -Mo<sub>2</sub>C/NC(NA),  $\beta$ -Mo<sub>2</sub>C/NC(SA).

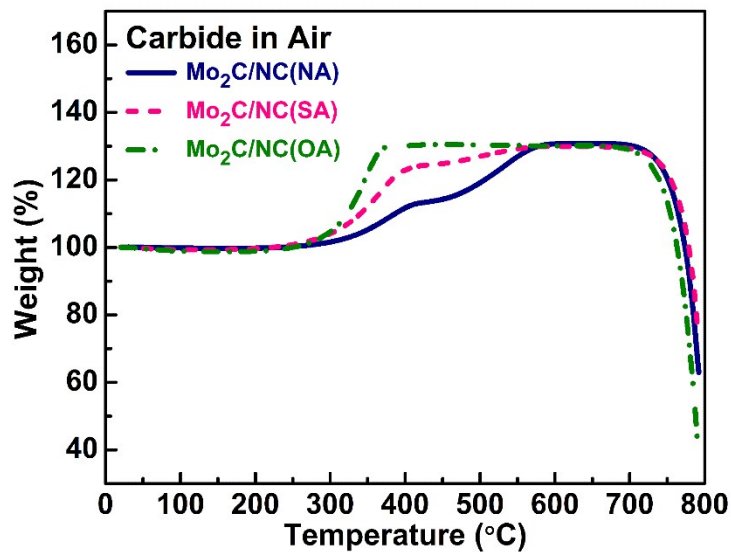


**Fig. S11** TGA curves for carbide of Mo<sub>2</sub>C/NC(OA), Mo<sub>2</sub>C/NC(SA), Mo<sub>2</sub>C/NC(NA).

As shown in Figure S10, Mo<sub>2</sub>C nanoparticles were oxidized to MoO<sub>3</sub> during the TGA measurement in oxygen atmosphere, followed by the consumption of carbon and dopants. When the temperature rises to 600°C, all the substances convert to only MoO<sub>3</sub>. The weight percent of Mo<sub>2</sub>C in as-prepared samples is estimated according to the following equation:

$$\begin{aligned}
 \text{m\% (Mo}_2\text{C)} &= \text{residual mass} * \text{M(Mo}_2\text{C)}/2\text{M(MoO}_3\text{)} \\
 &= 130.8 \text{ wt.\%} * 204/(2*144) = 92.6 \text{ wt.\%}
 \end{aligned}$$

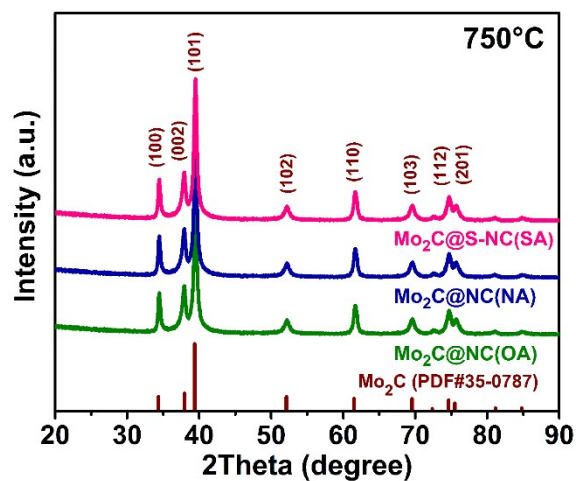




**Fig. S12** XRD patterns of  $\beta$ -Mo<sub>2</sub>C/NC(OA),  $\beta$ -Mo<sub>2</sub>C/NC(NA) and  $\beta$ -Mo<sub>2</sub>C/NC(SA) samples

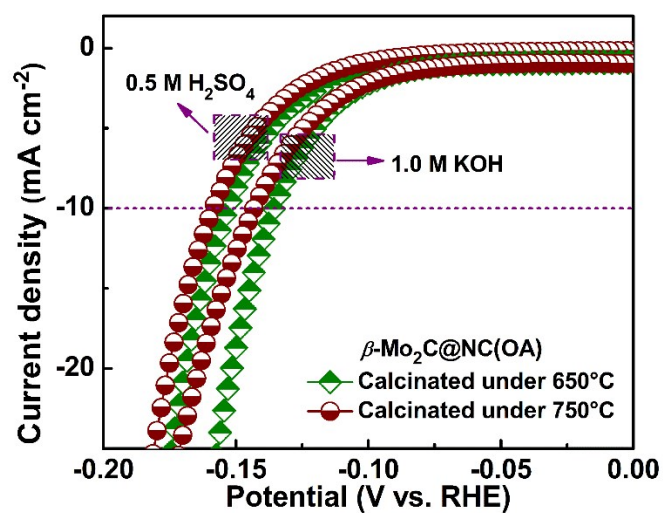


**Fig. S13** Polarization curves after *i*R correction in 0.5 M H<sub>2</sub>SO<sub>4</sub> (a) and 1.0 M KOH (b) for Mo<sub>2</sub>C/NC(OA) obtained at 650°C and 750°C.

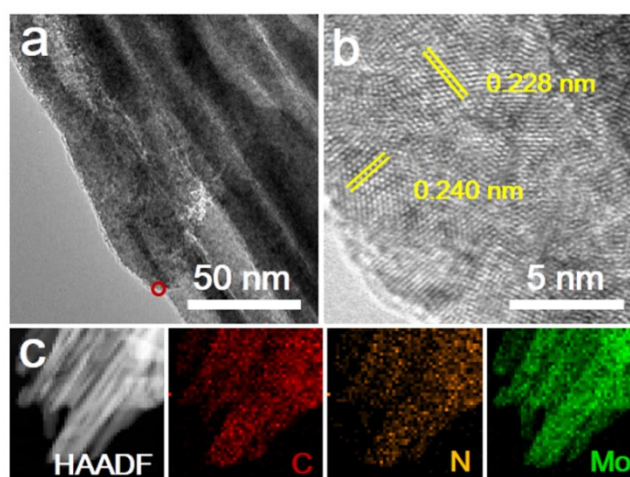


**Fig. S14** (a) TEM images, (b) HRTEM images, (c) HAADF and corresponding element mapping of  $\beta$ -Mo<sub>2</sub>C/NC(NA).



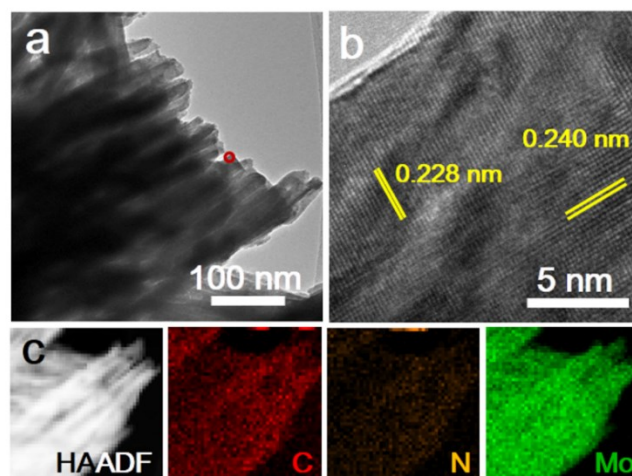


**Fig. S15** (a) TEM images, (b) HRTEM images, (c) HAADF and corresponding element mapping of  $\beta$ -Mo<sub>2</sub>C/NC(SA).

**Table S1.** Overpotential and Tafel slope of previously reported Mo<sub>2</sub>C-based electrocatalysts in acidic and alkaline condition.

Samples	Synthesize method	Mass loading (mg cm <sup>-2</sup> )	Overpotential(mV)		Tafel slope		Ref.
			(-10 mA cm <sup>-2</sup> )		(mV dec <sup>-1</sup> )		
			0.5 M	1.0 M	0.5 M	1.0 M	

			H <sub>2</sub> SO <sub>4</sub>	KOH	H <sub>2</sub> SO <sub>4</sub>	KOH	
$\beta$ -Mo <sub>2</sub> C-NC	Acid-Assisted	0.19	152	135	58	52	This work
Mo <sub>2</sub> C/NC-F	Dopamine-polymerized	0.28	144	100	55	65	S2
Mo <sub>2</sub> C nanobelts	Two-step	0.50	140	110	51.3	49.7	S3
Co <sub>4</sub> Mo <sub>2</sub> @NC	Physical mixing	0.35	-	218	-	73.5	S4
Pure $\beta$ -Mo <sub>2</sub> C	impregnation	1.0	-	130	-	66.5	S5
MoC-Mo <sub>2</sub> C/PN CDs	MOF-derived	0.40	-	121	-	60	S6
Mo/Co@N-C	MOF-derived	0.70	187	157	82	148	S7
NP-Mo <sub>2</sub> C	carburization	0.21	210	-	64	-	S8
Ni/Mo <sub>2</sub> C-NCNFs	electrospinning	1.4	195	143	77.4	57.8	S9
MoC-Mo <sub>2</sub> C	molybdate reacting with aniline	0.14	126	120	43	42	S10

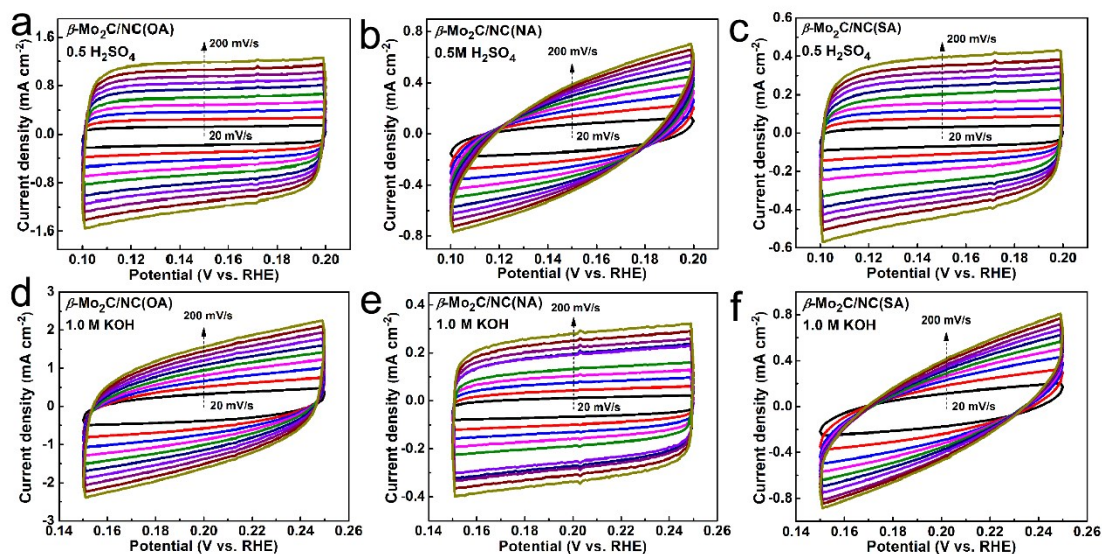


**Fig. S16** Cyclic voltammety curves of  $\beta$ -Mo<sub>2</sub>C/NC(OA),  $\beta$ -Mo<sub>2</sub>C/NC(SA),  $\beta$ -Mo<sub>2</sub>C/NC(NA) under different scan rate. These data were used to generate the plots showing the extraction of the  $C_{dl}$  for different samples shown in Figure 4 and Figure 5 in the main text.

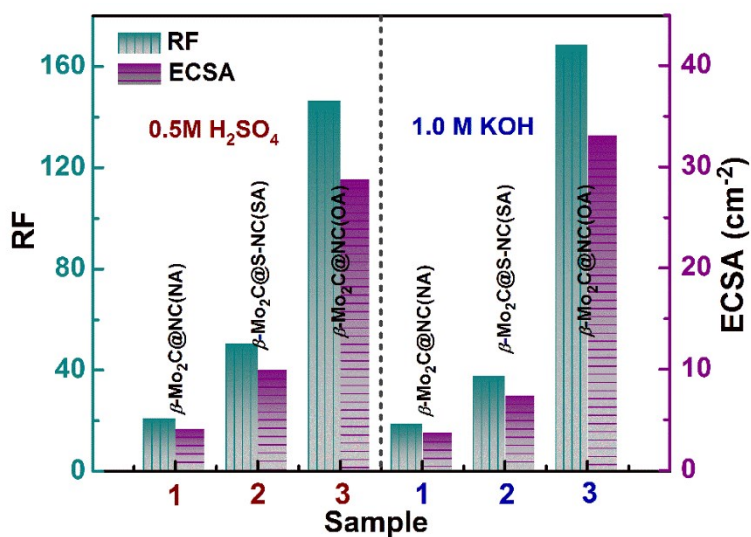


**Fig. S17** Comparison of the ECSA and RF for as-prepared catalysts

**ECSA calculation:**

$ECSA=C_{dl}/C_s$ , in which  $C_s$  is the specific capacitance, which is equal to 0.040 mF/cm<sup>2</sup> for a smooth electrode surface. Then the roughness factors (RF) were obtained by dividing the ECSA by the geometric area of the GCE.

**Table S2.** The fitting data of  $R_s$  and  $R_{ct}$  for as-prepared catalysts

Catalysts	0.5 M H <sub>2</sub> SO <sub>4</sub>		1.0 M KOH	
	$R_s$ ( $\Omega$ )	$R_{ct}$ ( $\Omega$ )	$R_s$ ( $\Omega$ )	$R_{ct}$ ( $\Omega$ )
$\beta$ -Mo <sub>2</sub> C/NC(OA)	5.44	0.45	5.87	0.38
$\beta$ -Mo <sub>2</sub> C/NC(SA)	7.43	1.86	6.32	1.87
$\beta$ -Mo <sub>2</sub> C/NC(NA)	5.14	3.07	5.56	1.55

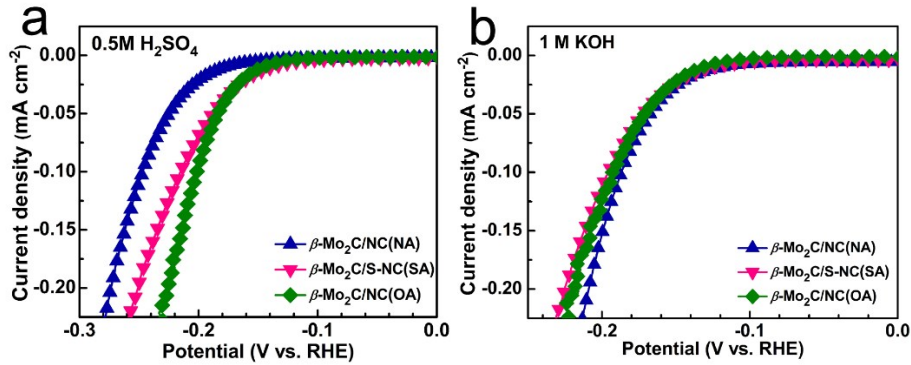


**Fig. S18** ECSA-calibrated LSV curves for as-prepared catalysts.

## References

S1. S. Q. Niu, S. W. Li, Y. C. Du, X. J. Han, P. Xu, How to reliably report the

overpotential of an electrocatalyst, *ACS Energy Lett.*, 2020, **5**, 1083–1087.

S2. Y. Huang, Q. F. Gong, X. N. Song, K. Feng, K. Q. Nie, F. P. Zhao, Y. Y. Wang, Min Zeng, J. Zhong, Y. G. Li, Mo<sub>2</sub>C nanoparticles dispersed on hierarchical carbon microflowers for efficient electrocatalytic hydrogen evolution, *ACS Nano*, 2016, **10**, 11337–11343.

S3. S. Y. Jing, L. S. Zhang, L. Luo, J. J. Lu, S. B. Yin, P. K. Shen, P. Tsiakaras, N-doped porous molybdenum carbide nanobelts as efficient catalysts for hydrogen evolution reaction, *Appl. Catal., B*, 2018, **224**, 533–540.

S4. J. Jiang, Q. X. Liu, C. M. Zeng, L. H. Ai, Cobalt/molybdenum carbide@N-doped carbon as a bifunctional electrocatalyst for hydrogen and oxygen evolution reactions, *J. Mater. Chem. A*, 2017, **5**, 16929.

S5. J. N. Xing, Y. Li, S. W. Guo, T. Jin, H. X. Li, Y. J. Wang, L. F. Jiao, Molybdenum carbide in-situ embedded into carbon nanosheets as efficient bifunctional electrocatalysts for overall water splitting, *Electrochim. Acta*, 2019, **298**, 305–312.

S6. X. F. Lu, L. Yu, J. T. Zhang, X. W. Lou, Ultrafine dual-phased carbide nanocrystals confined in porous nitrogen-doped carbon dodecahedrons for efficient hydrogen evolution reaction, *Adv. Mater.*, 2019, **30**, 1900699.

S7. C. Wu, D. Liu, H. Li, J. H. Li, Molybdenum carbide-decorated metallic cobalt@nitrogen-doped carbon polyhedrons for enhanced electrocatalytic hydrogen evolution, *Small*, 2018, **14**, 1704227.

S8. D. Z. Wang, T. Y. Liu, J. C. Wang, Z. Z. Wu, N, P (S) Co-doped Mo<sub>2</sub>C/C hybrid electrocatalysts for improved hydrogen generation, *Carbon*, 2018, **139**, 845–852.

S9. M. X. Li, Y. Zhu, H. Y. Wang, C. Wang, N. Pinna, X. F. Lu, Ni strongly coupled with Mo<sub>2</sub>C encapsulated in nitrogen-doped carbon nanofibers as robust bifunctional catalyst for overall water splitting, *Adv. Energy Mater.*, 2019, **9**, 1803185.

S10. H. L. Lin, Z. P. Shi, S. N. He, X. Yu, S. N. Wang, Q. S. Gao, Y. Tang, Heteronanowires of MoC–Mo<sub>2</sub>C as efficient electrocatalysts for hydrogen evolution reaction, *Chem. Sci.*, 2016, **7**, 3399.